Nuclear Materials Authority
P.O.Box 530 Maadi, Cairo, Egypt

ISSN 2314-5609
Nuclear Sciences Scientific Journal
vol. 2, p 55 - 68
2013

GEOLOGY AND URANIUM, THORIUM DISTRIBUTIONS OF GABAL HUMR AR-RAHA AREA, NORTH EASTERN DESERT, EGYPT

AHMED A. ABU STEET
Nuclear Materials Authority, Cairo, Egypt

ABSTRACT

Gabal Humr ar-Raha area, about 150 km^2 of crystalline basement rocks, is delineated by Lat. 27^o $18'$ and 27^o $26'$ N and Long. 32^o $42'$ and 32^o $48'$ E. It is covered by Dokhan volcanics (oldest), younger granites (syenogranite) and post granitic dykes (youngest).

Dokhan volcanics are represented by a thick sequence of stratified lava flows of intermediate (andesites) and acidic (rhyolites) composition. The main rock type of Gabal Humr ar-Raha granitoid rocks are classified as syenogranites; their emplacement were structurally controlled by pre-existing fractures trending NNE-SSW and NE-SW.

The acidic Dokhan volcanics and younger granites show the highest equivalent uranium and equivalent thorium contents in the study area. The younger granites can be considered as uraniferous granites as revealed from their radiometric studies. They are originated from highly fractionated U-rich magma that trapping high concentrations of uranium in the accessory minerals. These granites host an interesting radioactive anomalies which are essentially exhibited by a strongly altered granites occupying at the intersection zone of two major strike-slip faults striking NNW-SSE and NE-SW. The sheared granites show dark brown spots of iron oxides at this zone. Thus the enrichment of uranium in the study area is controlled by structural elements.

INTRODUCTION

The basement rocks of Egypt cover about 100 000 km^2 (about 10 % of the total area of Egypt). Granitoids constitute an important rock group covering vast areas of the Arabian-Nubian Shield. They cover about 38 % of the basement rocks in Egypt. In the north Eastern Desert of Egypt, the Pre-Cambrian rocks are dominated by Dokhan volcanics (D.V) and granitoids (Basta et al., 1980; Greenberg, 1981; Dardir et al., 1982; Stern and Gottfried, 1986; Wetait, 1997 and Ayoub and Moharem, 2008).

The Egyptian granitoids have received particular attention by many workers and are broadly distinguished into two main categories, the older and younger granitoids; each category is subdivided in different ways. They are classified according to their type localities (Shaitian and Gattarian, Hume, 1935), relative age (older and younger granites, El-Ramly and Akaad, 1960), their apparent relation to Orogeny (Syn-, Late- and Post-Orogenic, El-Shazly, 1964) and also according to their geochemical characteristics (calc-alkaline, alkaline to per-akaline granites, El-Gaby, 1975), mineralogical, textural and chemical characteristics (Greenberg, 1981), orogeny (Hussein et. al., 1982), age and orogeny (El-Shatoury et al., 1984), origin and tectonic setting (Kabesh et al., 1987), the difference in mineralogical composition (El-Gaby et al., 1990), petrological and geochemical criteria (Noweir et al., 1990).

In spite of the accessibility of the present area, few workers had contributed to its regional geology. Hume, (1934) gave a generalized geological map of the Eastern Desert of Egypt. El-Ramly, (1972) compiled a regional geologic map for the basement rocks in the Eastern and south Western Desert of Egypt. Dardir and Abu Zeid, (1972) mapped an area between Lat. 27^{o} 00' and 27^{o} 30' N. Abu El Leil, (1980) described the geology of the northern part of the Eastern Desert of Egypt and classified the rocks as follows: Syn-orogenic stage (quartz-diorite), Late-orogenic stage (granites) and Post-granitic stage (dyke rocks). Ayoub, (2003) studied the petrogenetic implications of the Umm Tweir granitoid rocks and stated that the analyzed syenogranites fall within the calc-alkaline I-type granitoid field; and is associated with radioactive anomalies concentrated along fault planes and shear zones.

The present paper aims to give detailed geological and radioactive studies of the different rock types exposed at Gabal Humr ar-Raha area.

GEOLOGIC SETTING

Gabal Humr ar-Raha area covers about 150 km^2 of crystalline basement rocks, located west of Gabal Umm Tweir, along Wadi Giala and Wadi Lissan El-Baqara, about 150 km west Hurghada in the northern part of the Eastern Desert, delineated by lat. 27^{o} 18' and 27^{o} 26' N and long. 32^{o} 42' and 32^{o} 48' E (Fig.1). The area is covered by Dokhan volcanics (oldest), younger granites (syenogranite) and post granitic dykes (youngest).

Lithology

The Dokhan volcanics (D.V) are widely distributed through G. Humer ar-Raha area and form an elongated belt of moderate elevation in NE-SW direction, rise up to 588 m above sea level (a.s.l.); as well as small isolated outcrops. They are represented by thick sequence of stratified lava flows of intermediate to acidic composition. They are associated with few intercalations of pyroclastics represented mainly by welded ash flow tuffs, lapilli and crystal tuffs as well as vitric ryholitic tuffs increasing westward. Lapilli and ash tuffs sometimes show graded bedding and lamination.

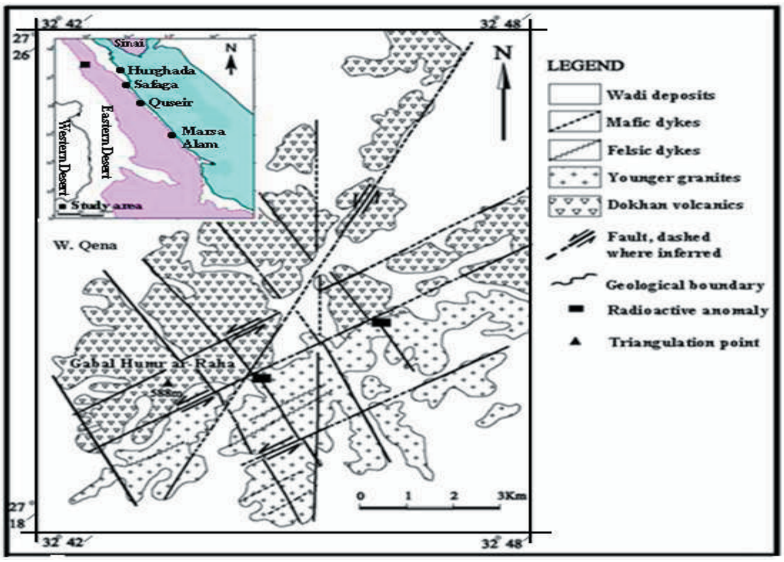

Fig. 1: Geologic map of Gabal Humr ar-Raha area, North Eastern Desert, Egypt

The lava flows are pale grey to dark grey in colour and range in composition from andesite to rhyolite. Porphyritic texture is well developed in most of these rocks, while few of them are non-porphyritic and some are amygdaloidal. The amygdals are filled with quartz and carbonates. These rocks are well represented at Gabal Humr ar-Raha near the syenogranites where they change gradually upward from non-porphyritic andesite to porphyritic varieties. The main alteration processes affected these rocks are chloritization, sericitization and silicification.

Sometimes, they comprise lapillis of different sizes, shapes and composition. The Dokhan volcanics are particularly, unfolded but often tilted, broken and crushed especially near their contact with the younger granites and fault planes.

The younger granites are situated at the southern part of the mapped area. They form few individual bodies as stocks of low to moderately high relief. At south-east of G. Humr ar-Raha, the younger granites form an elongated shaped pluton with low to moderately hilly country of bright reddish pink colour. Their red colour is essentially due to their high contents of potash feldspars and the staining by secondary red hematitic materials particularly along their joints. They are commonly medium- to coarse-grained, hard, massive and compact, rich in quartz and potash feldspars but poor in mafics (they range in composition from varieties that contain no or little mafics to varieties carrying notable amounts of biotite).

These granites intrude the Dokhan volcanics with sharp intrusive contact (Fig. 2) and send few apophyses and tongues in some parts through them. They catch xenoliths of Dokhan volcanics of different shapes and diameters (Fig. 3) and sometimes the Dokhan volcanics overlying them as roof- pendants. They show well marked exfoliation essentially controlled by the topographic surfaces of rocks (Fig. 4).

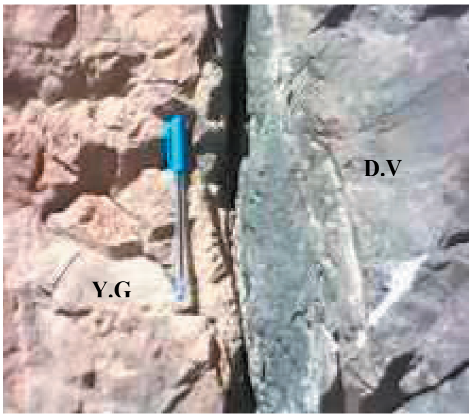

Fig. 2: Close up view showing Dokhan volcanics (D.V) intruded by younger granites (Y.G) with sharp intrusive contact, looking NW

Fig. 3: Close up view showing xenolith of Dokhan volcanics within younger granites, G. Humr ar-Raha, looking N

Fig. 4: Close up view showing exfoliation in younger granites, looking NE

Generally, these younger granites are characterized by cavernous and bouldery weathering (Fig. 5). They are porphyritic to equigranular and massive. They contain some quartz veins and feldspar filling joints, fault planes and fractured zones (Fig 6). These veins trending mostly in the NE-SW and E-W directions with vertical or steep dips. Moreover, these younger granites are characterized by the common presence of pegmatitic dykes and pockets (Fig. 7). The pegmatites are mainly of unzoned type and composed of milky quartz and reddish pink K-feldspars with or without mica.

Fig. 5: Younger granites showing cavernous weathering, looking SE

Fig. 6: Close up view showing quartz vein filling joints in younger granites, looking NE

Fig. 7: Close up view showing pegmatite dyke cuts in younger granites, looking E

Post granitic dykes (felsic and mafic) cutting all the previously described rocks and forming prominent high ridges trending along NE-SW. The felsic dykes are the older one, mainly striking in NE-SW and ENE-WSW directions with vertical or steep dips to NW and SSE and may extend for several kilometers. The mafic dykes strike in NE-SW with similar dips as the felsic dykes.

Structures

Primary and secondary structures are well visible in the study area. Primary structures include volcanic flows, graded bedding, lamination and bedding in Dokhan volcanics. Secondary structures include joints and faults.

Around G. Humr ar-Raha area, the main trend of the bedding plane of Dokhan volcanics varies from NNW-SSE to NE-SW, dipping westwards at angle ranging from 10^{o} to 15^{o}. The angle of dip is usually increasing toward the contact with the granite mass; it sometimes reaches up to 25^{o} at the contact zone due to the emplacement force.

Joints are recorded in all rock types. They are mainly tension and subordinate shear joints. The most common directions of joints in the Dokhan volcanics, in decreasing order of predominance are NW-SE, NE-SW and N-S and dipping 80^{o}-85^{o} to SW, 75^{o}-80^{o} to NW and 75^{o}-88^{o} to E respectively (Fig. 8a). In younger granites, the main joint trends, in decreasing order of predominance, are ENE-WSW, NE-SW and E-W and dipping 75°-88° to SSE, 75°-85° to SE and 70°-80° to S respectively (Fig. 8b).

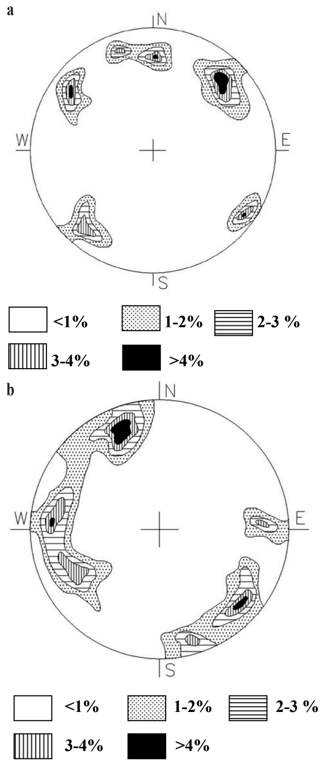

Fig.8 :Contour diagram of joint poles in the Dokhan volcanics (a) and younger granites (b)

Faults in the area have two main trends, being the NNW-SSE and NE-SW (Fig.9). The NNW-SSE shear zones and faults show dextral displacement and is a principal complementary shear to the NE-SW sinistral faults and shear zones. The exact attitude of the first group trend N15°W-S15°E with 17° ENE plunging slickensides while the other group is trending N35°E-S35°W with 22° SE plunging slickensides. The calculated maximum principal stress (σ1) causing these shear zones is trending N10°E with 7° plunging while the minimum principal stress (σ3) is vertically acting with 83° steep plunging. The strain ellipse demonstrating this deformation is shown on Figure (10).

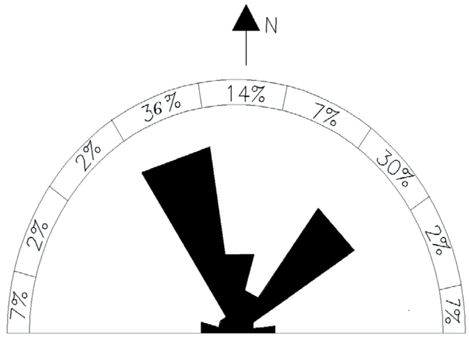

Fig. 9 : Rose diagram showing the main directional trends of fault lines according to their number

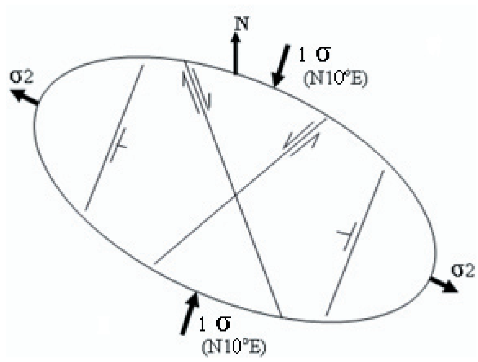

Fig.10: Strain ellipse demonstrating the deformation in the area

These two main trends (NE-SW and NNW-SSE) are matched with the faults of Yossef, (1968); Garson and Krs, (1976); Meshref, (1990); Shalaby, (1996) and Ayoub, (2003).

PETROGRAPHY

Dokhan Volcanics

The Dokhan volcanics are mainly andesites and rhyolites. Andesites are mainly porphyritic and composed of plagioclase, hornblende, biotite and small amount of quartz phenocrysts embedded in fine-grained groundmass. Apatite and iron oxides are accessory minerals while epidote, chlorite and clay minerals are alteration products. Plagioclase is of andesine composition (An35-45) as anhedral to subhedral phenocrysts exhibiting simple and lamellar twinning (Fig. 11). They are arranged in subparallel orientation, suggesting flow texture. These phenocrysts are partly altered to saussurite, chlorite and epidote (Fig.12). Hornblende occurs as subhedral prismatic phenocrysts that are strongly pleochroic from pale to dark green colour. Some hornblende crystals show simple twinning (Fig.13). Biotite flakes and quartz are present in small amounts commonly disseminated in the groundmass. Rhyolite is essentially composed of sanidine, quartz and muscovite. Zircon and iron oxides occur as accessory minerals. Sanidine occurs as phenocrysts usually twinned (Fig.14). Quartz crystals are highly corroded and invaded by the groundmass. Muscovite appears as irregular flakes corroded by quartz and feldspar phenocrysts. The Dokhan volcanic rocks have suffered from low grade regional metamorphism (lower green-schist facies) as indicated from the replacement of hornblende and biotite by chlorite, epidote and iron oxides.

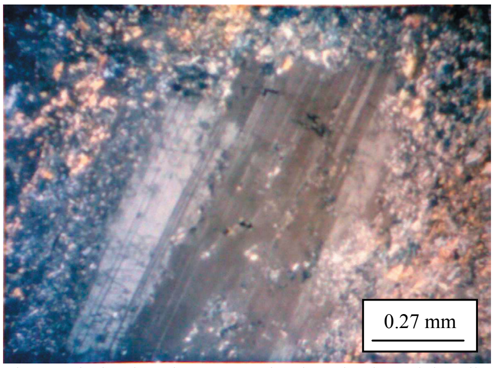

Fig.11: Plagiocalse phenocrysts showing simple and lamellar twinning, porphyritic andesite, xpl

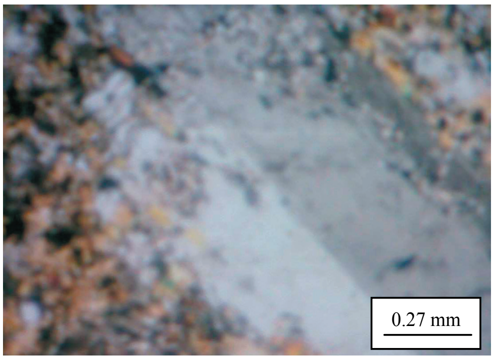

Fig.12: Plagioclase phenocrysts partly altered to saussurite, porphyritic andesite, xpl

Fig.13: Hornblende phenocryst showing simple twinning, porphyritic andesite, xpl

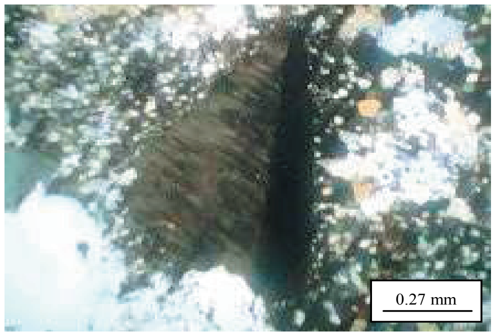

Fig.14: Sanidine phenocryst showing simple twinning, rhyolite, xpl

Younger Granites

Modal analyses of the studied younger granites (Table 1) are plotted on Q-A-P diagram of Streckeisen (1976). These younger granites are plotted in the syenogranite field (Fig.15).

The syenogranites are mainly composed of potash feldspars, quartz, plagioclase, biotite and muscovite as essential minerals (Fig.16). Zircon, sphene, allanite and apatite are the main accessory minerals. Clay minerals, epidote, zoisite, iron oxides and muscovite are secondary minerals. Potash feldspars are represented by orthoclase and microcline perthites but orthoclase perthite is the predominant. They are generally of string, patchy and/or flame-like types. They are corroded by quartz and muscovite. Quartz occurs as subhedral to anhedral crystals of variable shapes and sizes. Some quartz crystals show undulose extinction, indicating high strain effects.

Plagioclase is found as subhedral to euhedral albite-oligoclase crystals (An_{5-15}) showing simple and lamellar twinning and partly altered to epidote and zoisite. Biotite occurs as small flakes that may enclose zircon crystals. Zircon is found as prismatic euhedral to subhedral crystals included in quartz and biotite. Some zircon crystals are occasionally surrounded by strong pleochroic halos due to radiogenic effects (Fig. 17). Sphene (titanite) occurs as sphenoid euhedral to anhedral crystals corroded by feldspars and quartz (Fig. 18). Apatite is found as minute euhedral prismatic and needle-like crystals included in feldspars, biotite and quartz. Allanite occurs as euhedral prismatic crystals showing strong pleochroism from buff to deep reddish brown (Fig.19). Iron oxides are found as small irregular patches.

Table 1: Modal analyses of the studied younger granites of Gabal Humr ar-Raha area

Sp.No.	Mineral composition				
	Quartz	K-feldspar	Plagiocalse	Biotite	Accessories and opaques
1	35.15	43.18	17.21	2.17	2.29
2	29.72	46.57	17.92	3.15	2.64
3	30.85	48.98	14.95	3.11	2.11
4	27.52	46.23	21.62	2.12	2.51
5	31.16	51.51	13.11	2.21	2.01
6	22.95	47.87	23.90	3.14	2.14
7	27.02	49.12	19.13	2.15	2.58
8	30.68	45.11	19.35	2.17	2..09

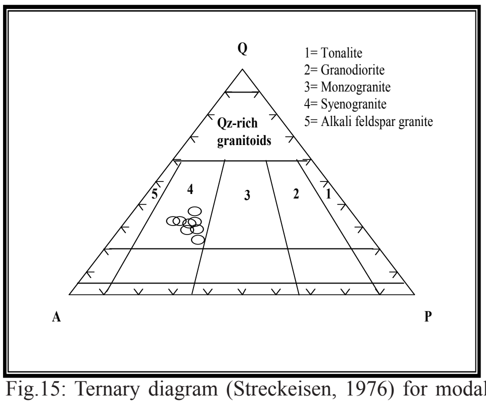

Fig.15: Ternary diagram (Streckeisen, 1976) for modal quartz (Q), alkali feldspar (A) and plagioclase (P) of the studied younger granites

Fig.16: Syenogranite showing potash feldspars, quartz, plagioclase and biotite as essential minerals, xpl

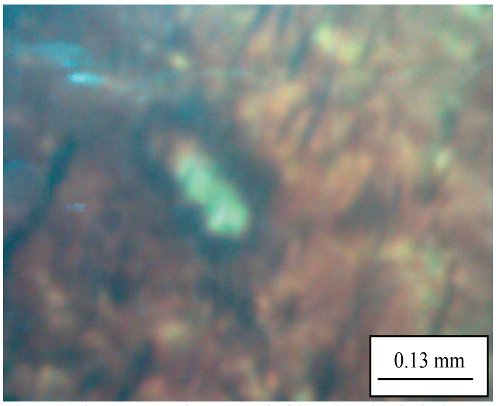

Fig.17: Zircon crystal surrounded by pleochroic halo, syenogranites, xpl

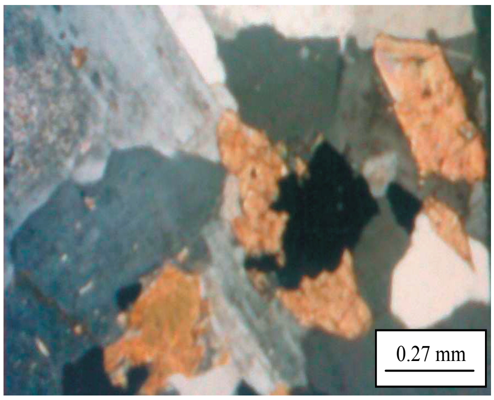

Fig.18: Titanite with characteristic sphenoid shape corroded by quartz and feldspars in syenogranites, xpl

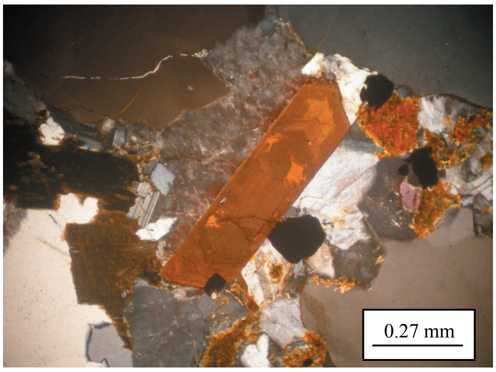

Fig.19: Allanite crystal in syenogranite, xpl

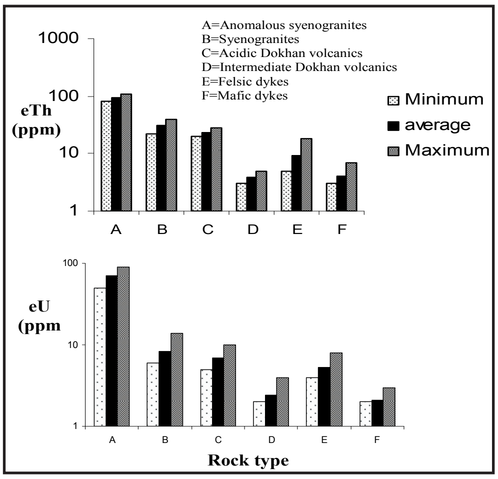

Fig.20 : Comparative histogram showing the distribution of radioactivity level (ppm) in the various rocks of G. Humr ar-Raha area

RADIOACTIVITY

The radioactivity of the different rock types in the study area were measured for the equivalent uranium (eU) and equivalent thorium (eTh) in part per million (ppm) using portable gamma ray spectrometer UG-130. The ranges of normal radioactivity values for the different rock types are summarized in Table (2) and graphically represented on Figure (20).

Table 2: Field gamma-ray radioactivity (ppm) for all rock types exposed in Gabal Humr ar-Raha area using a portable gamma-ray scintillometer (UG-130)

Rock type	No. measurements	eU (ppm) Range	eU (ppm) Average	eTh (ppm) Range	eTh (ppm) Average
Anomalous syenogranite	15	50 - 90	70.8	80 - 110	92.1
Normal syenogranites	60	6 - 14	8.3	22 - 40	30.7
Acidic Dokhan volcanics	20	5 - 10	6.9	20 - 28	23.6
Intermediate Dokhan volcanics	30	2 - 4	2.4	3 - 5	3.8
Felsic dykes	10	4 - 8	5.3	5 - 18	9.4
Mafic dykes	15	2 - 3	2.1	3 - 7	4.1

From the field radiometric survey measurements and the distribution of radioactivity values, it is clear that the syenogranites and the acidic Dokhan volcanics possess the highest level of eU and eTh among the various rock types cropping out in the study area. The eU of the fresh coarse- to medium-grained syenogranite of G. Humr ar-Raha ranges between 6 pm and 14 ppm with an average 8.3 ppm and eTh from 22 ppm to 40 ppm with an average 30.7 ppm. The eU of the acidic Dokhan volcanics ranges between 5 ppm and 10 ppm with an average 6.9 ppm and eTh from 20 ppm to 28 ppm with an average 23.6 ppm (Table 2). This indicates that, the studied syenogranites and acidic Dokhan volcanics are originated from highly fractionated U-rich magma and trapping high concentrations of uranium in accessory minerals.

The syenogranite of G. Humr ar-Raha hosts an interesting radioactive anomaly that is located in the southern part of G. Humr ar-Raha along a small tributary branched from the only accessible narrow wadi traversing this granitic pluton at its contact with the Dokhan volcanic rocks. It is essentially exhibited by a strongly sheared granitic zone (about 2x7m dimensions) following the intersection zone of two major strike-slip faults striking NNW-

SSE and NE-SW. The younger granites near this zone show 10 ppm eU and 25 ppm eTh, while at the radioactive zone it rises to 75 ppm eU and 90 ppm eTh reaching up to 90 ppm eU and 110 ppm eTh after digging for 20 cm, where numerous concentrations of dark brown spots of iron oxides are noticed. The granites at this zone are highly sheared, medium- to fine-grained and red to reddish brown colour due to the strong hematitization.

The analyzed grab sample that collected from this sheared granitic zone has average eU content 66.3 ppm and average eTh content 104 ppm, while the average eTh/eU ratio is 1.57 (Table 3). This indicates strong post-magmatic uranium enrichment in this location by hydrothermal solution. The extensive hematitization caused the adsorption of uranium from these circulating solutions.

Table 3: eU, eTh, eTh/eU and Zr of the studied rocks, Gabal Humr ar-Raha area

Rock type	Sp. No.	eU (ppm)	eTh (ppm)	eTh/eU	Zr
	1	11.4	35.5	3.11	232
Normal	2	09.8	28.7	2.92	218
syenogranite	3	12.4	38.8	3.12	240
	4	10.3	29.8	2.89	225
	5	13.2	39.1	2.96	246
	6	14.6	40.1	2.74	248
Average		11.95	35.33	2.95	234.83
Anomalous	7	70.3	110.4	1.57	447
syenogranite	8	62.3	98.5	1.58	435
Average		66.3	104.45	1.57	441
Acidic Dokhan	9	9.3	28.2	3.03	195
volcanics	10	10.4	31.1	2.99	210
(rhyolites)	11	7.8	25.4	3.25	185
	12	8.2	26.9	3.28	190
	13	9.7	29.5	3.04	200
	14	10.1	30.2	2.99	207
Average		9.25	28.55	3.09	197.83
	15	1.6	4.6	2.88	189
Intermediate	16	1.8	5.1	2.83	192
Dokhan	17	1.4	4.5	3.21	201
volcanics	18	1.7	5.0	2.94	185
(andesites)	19	1.5	4.4	2.93	182
	20	1.3	4.1	3.15	187
Average		1.55	4.61	2.99	189.33

From Tables (2&3), it is noticed that the Lab. measurements are usually similar to the field measurements suggesting that the UG-130 instrument is well calibrated and the field measurements are dependable.

Inter-Element Relationships

The increase in eU and eTh contents is parallel to the line of differentiation of these granites. This is expected because both U and Th are incompatible trace elements with the major rock-forming minerals.

The results of the radiometric analysis of eU and eTh of the studied younger granites are given in Table (3). The relationship between eU and eTh may indicate the enrichment or depletion of U because Th is chemically stable. Normally, thorium is three times as abundant as uranium in all rock types (Darnley, 1982). When this ratio is disturbed, it indicates either depletion or enrichment of uranium (Cambon, 1994). A positive correlation between equivalent uranium and equivalent thorium for each rock type on the constructed diagram (Fig.21) revealing that their behavior was probably controlled by magmatic processes (Simpson et al., 1979).

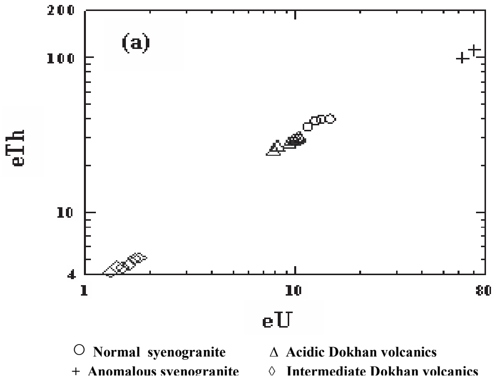

Fig.21: eU (ppm) versus eTh (ppm) variation diagram

The poor relationship between eU and eTh/eU (Fig.22) indicates that uranium distribution within these rocks is not only controlled by magmatic processes but also by secondary processes to a great extent, where the anomalous syenogranites show enrichment of uranium while the Dokhan volcanics show variable degrees of U-leaching. The positive correlation between eU and Zr (Fig.23) supports the concept that uranium was trapped in the accessory minerals as zircon. Accordingly, Humr ar-Raha granitic pluton is not only originated from U-rich magma, but also have suffered from secondary processes which added uranium in metamict zircon, allanite and iron oxyhydroxides to adsorb uranium from circulating solutions. Table (3) shows that, the eTh/eU ratios for the studied anomalous syenogranites are lower than that given by Tammemagi and Smith (1975) which range from 3 to 4 for the normal granites. This means the enrichment of uranium relative to thorium in the studied granites.

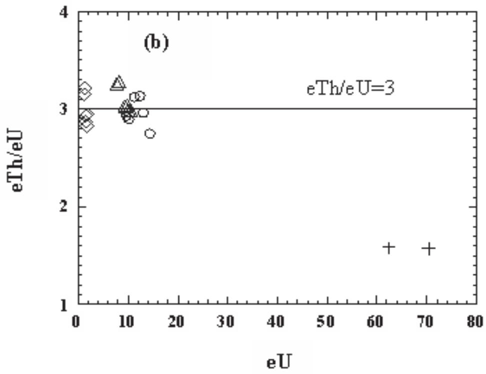

Fig. 22: eU (ppm) versus eTh/eU variation diagram, Symboles as in Fig. 21

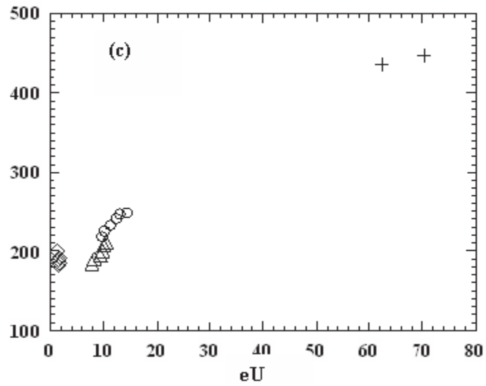

Fig. 23: eU (ppm) versus Zr (ppm) variation diagram, Symboles as in Fig. 21

The mineralogical studies reveal that the high uranium content in the anomalous syenogranites is related to their zircon and allanite contents. The anomalous syenogranite samples were subjected to heavy liquid separation and picking. The separated zircon forms euhedral to subhedral crystals (Figs.24&25) where their size ranges from about 30 to 140 µm. They were analyzed using Environmental Scanning Electron Microscope (ESEM). The obtained analysis clarified presence of the radio-elements (U and Th) in the structure of zircon (Fig.26).

Fig.24: General view of separated zircon from anomalous syenogranites

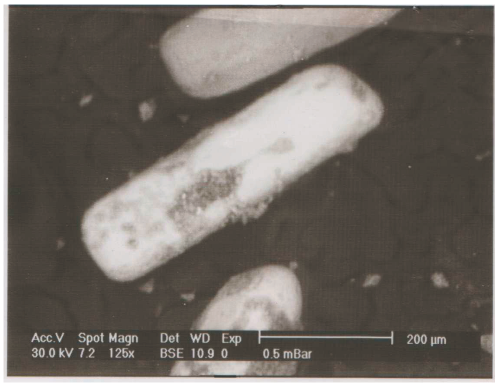

Fig. 25: BSE image of zircon

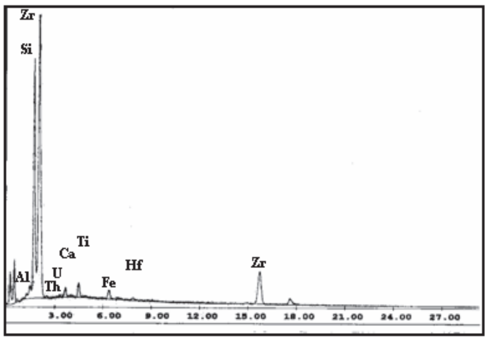

Fig.26: EDX spectra of zircon

Allanite [Ca (Ce,La,Y)$_2$ Fe$_2$Al$_3$ (O/OH/SiO/Si$_2$O$_7$)] forms anhedral to subhedral crystals (Figs.27&28). They were analyzed using Environmental Scanning Electron Microscope (ESEM). The obtained analyses clarified presence of radio-elements (U and Th) in the structure of allanite (Fig.29). The studied allanite exhibits enrichment of light rare earth elements (LREE) indicating syngenetic allanite (El-Balakssy et al., 2011). The presence of Ce-rich allanite indicates much-localized remobilization and concentration of REE during a late hydrothermal alteration (Yuanming and Michael, 1991).

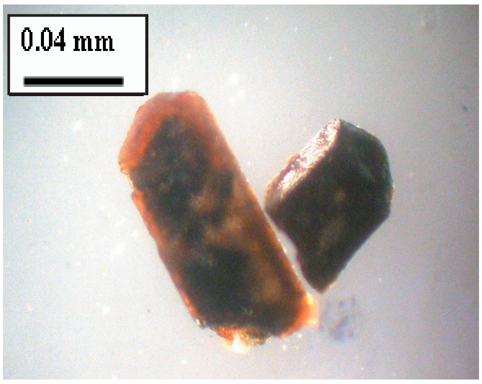

Fig.27: General view of separated allanite from anomalous syenogranites

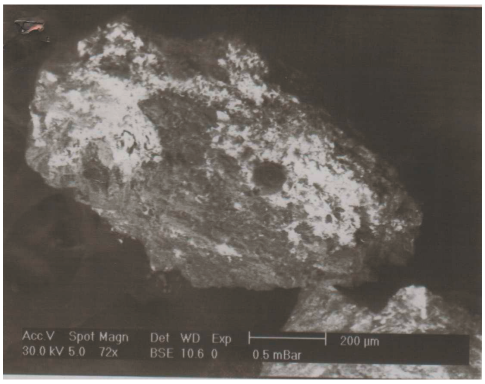

Fig. 28: BSE image of allanite

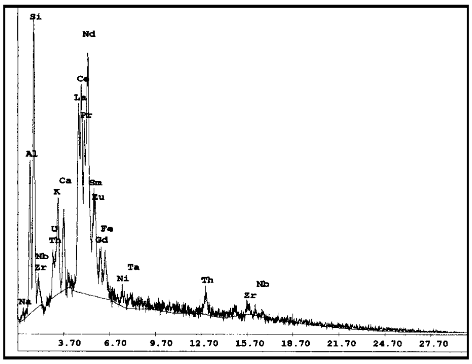

Fig. 29: EDX spectra of allanite

SUMMARY AND CONCLUSIONS

The field radiometric survey and structural studies of joints showed that their radioactivity is normal, whereas the radioactivity readings measured on joints filled with K-feldspars or strongly hematitized are relatively higher than the barren joints. This phenomenon is often attributed to the effect of K^{40} isotope of the potash feldspars on the radioactivity of the rocks (Heinrich, 1958). On the other hand, iron oxides are sometimes abnormally radioactive due to their high ability to capture uranium from its circulating fluids (Rogers et al., 1978).

Concerning faults, it is observed that, the distribution of the majority of the radioactive anomalies is controlled by some major faults especially the NE-SW fault sets and their associated shear zones. They play an important role in controlling most of the recorded radioactive anomalies. This trend is considered as the most radioactive direction if compared with the other fault sets recorded in the study area. It is also observed that, the zone of intersection of faults striking NE-SW with those belonging to the NNW-SSE trend are relatively of high gamma radioactivity. The increase of radioactivity at the intersection zone of faults may be due to the brecciated and sheared zones which act as pathway for the circulating hydrothermal solutions bearing radioelements and the localization of radioactive anomalies.

The analyzed grab samples, collected from this sheared granitic zone have average eU content 66.3 ppm and average eTh content 104 ppm, while the average eTh/eU ratio is 1.57. This indicates strong post-magmatic uranium enrichment in this location by hydrothermal solutions. The enrichment of uranium by secondary processes than magmatic crystallization is usually controlled by structural elements. Faults, fractures and joints play an important role as they act as pathways or channels for the circulating hydrothermal solutions.

The poor relationship between eU-eTh/eU indicates that uranium distribution within these rocks is not only controlled by magmatic processes but also by secondary processes to a great extent. The positive correlation between eU and Zr supports the concept that uranium was trapped in the accessory minerals as zircon. The mineralogical studies reveal that the high uranium content in the anomalous syenogranites is related to their zircon and allanite content.

REFERENCES

Abu El-Leil, I.,1980. Geology, petrography and geochemistry of some granitic rocks in the north part of the Eastern Desert of Egypt. Ph. D. Thesis, Al Azhar Univ., Egypt, 294 p.

Ayoub, R.R.,2003. Geology and radioactivity of Gabal Um Tweir area, North Eastern Desert, Egypt. Ph. D. Thesis, Cairo Univ., Egypt, 286 p.

Ayoub, R. R., and Moharem, A. F.,2008. Petrology and distribution of uranium in the younger granites of Esh El-Mallaha Range, North Eastern Desert, Egypt. Al-Azhar University, Egypt. 6th Al-Azhar Inter. Sci. Conf. (AISC'08).

Basta, E.Z.; Kotb, H., and Awadallah, M.F.,1980. Petrochemical and geochemical characteristics of the Dokhan Formation at the type locality, Gebel Dokhan, Eastern Desert, Egypt. IAG Bull. Jeddah, 3,122 - 140.

Cambon, A.R.,1994. Uranium deposits in granitic rocks. Notes on the national training course on uranium geology and exploration. Organized by IAEA and NMA, 8 - 20 Jan. 1994.

Darnley, A.G.,1982. "Hot granites" Some general remarks, In: Uranium in granites (Maurice, Y. J. , ed.). Geol. Surv. Canada, paper No. 81 - 23, 1 - 10.

Dardir, A.A., and Abu Zeid, K.M.,1972. Geology of the basement rocks between Lat. 27o 00' and 27o 30' N, Eastern Desert. Ann. Geol. Surv. Egypt, II,129-159.

Dardir, A.A.; Awadallah, M.F., and Abu Zeid, K.M.,1982. A new contribution to the geology of Gebel Dokhan, Eastern Desert, Egypt. Ann. Geol. Surv. Egypt, XII,19-27.

El-Balakssy, S.S.; Saleh, W. H., and El-Husseiny, M. O.,2011. Characterization of accessory allanite from Um Lassifa granites, Central Eastern Desert, Egypt. (in press)

El-Gaby, S.,1975. Petrochemistry of some granites from Egypt. N.Jb. Miner. Abh.,124,147 - 189.

El-Gaby, S.; List, F.K., and Tehrani, R.,1990. The basement complex of the Eastern Desert and Sinai. In Said, R. (ed.); The Geology of Egypt. Balkema, Rotterdam,175 - 184.

El-Ramly, M.F.,1972. A new geological map for the basement rocks in the Eastern and south Western Desert of Egypt (scale 1: 1000,000). Ann. Geol. Surv. Egypt,II, 1- 18.

El-Ramly, M.F., and Akaad, M.K.,1960. The basement complex in the central Eastern Desert of Egypt between Lat. 24o 30' and 25o 40' N. Geol. Surv. Cairo, 8, 35 p.

El-Shatoury, H.M.; Mostafa, M.E., and Nasr, F.E.,1984. Granites and granitoid rocks in Egypt - a statistical approach of classification. Chem. Erde,43, 83 - 111.

El-Shazly, E.M.,1964. On the classification of the Precambrian and other rocks of magmatic affiliation in Egypt. 22nd Int. Geol. Congr. Proc. Sect. 10, India,88 - 101.

Garson, M.S., and Krs, M.,1976. Geophysical and geological evidence of the relationship of Red Sea transverse tectonics to ancient fractures. Bull. Geol. Soc. Am.,87, 169 - 181.

Greenberg, J.K.,1981. Characteristics and origin of Egyptian younger granites. Geol. Soc. Amer. Bull. part II, 92,749 - 840.

Heinrich, F.W.,1958. Mineralogy of radioactive raw materials. McGraw Hill Book Co., New York, 654 p.

Hume, W.F.,1934. Geology of Egypt. Geol. Surv. Egypt, Government press, Cairo,II, Part I, 1 - 300.

Hume, W.F.,1935. Geology of Egypt. Geol. Surv. Egypt, Government press, Cairo,2 (2), 301 - 688.

Hussein, A.A.; Ali, M.M., and El Ramly. M.F.,1982. A proposed new classification of the granites of Egypt. J. Volc. anal. Geoth. Erm. Res. ,14,187 - 198.

Kabesh, M.L.; Salem, A.K.A., and El-Sheshtawi, Y.A.,1987. On the chemical behaviour, origin and tectonic setting of some younger granitoids, Eastern Desert, Egypt. Bull. Fac. Sci. Zagazig Univ. , 9, 300 - 336.

Meshref, W.M.,1990. Tectonic framework of Egypt. In: geology of Egypt (Said, R., ed.). 113 - 155.

Noweir, A. M.; Sewifi, B. M., and Abu El Ela, A. M.,1990. Geology, petrography, geochemistry and petrogenesis of the Egyptian younger granites. Qatar Univ. Bull., 10, 363-393.

Rogers, J.W.; Ragland, P.C.; Nishimori, R.K.; Greenberg, J.K., and Hauck, S.A.,1978. Varieties of granitic uranium deposits and favourable exploration areas in the Eastern United States. Econ. Geol.,73,1539 - 1555.

Shalaby, M.H.,1996. Structural controls of uranium mineralizations at Gabal Qattar,. north Eastern Desert, Egypt. Proc. Egypt. Acad Sci., 46, 521-536.

Simpson, G. M.; Lee, J. H.;Zoubok, B., 1979. A rating scale for tardive dyskinesia. Psychopharmacology, 64, 171–179.

Stern, R.J., and Gottfried, D.G.,1986. Petrogenesis of a late Precambrian (575-600 Ma) bimodal suite in northeast Africa. Contrib. Mineral. Petrol., 92, 492-501.

Streckeisen, A.,1976. To each plutonic rock its proper name. Earth Sci. Rev.,12,1 - 33.

Tammemagi, H.Y., and Smith, N.L.,1975. A radiogeologic study of the granites of SW England. J. Geol. Soc. London, 131(4), 415-427.

Wetait, M.A.,1997. Petrology, geochemistry and tectonic evolution of the Pan-African rocks of Wadi Um Balad-Wadi El Urf area, north Eastern Desert, Egypt. Egypt. J. Geol., 41/2B, 431 - 455.

Youssef, M.I.,1968. Structural pattern of Egypt and its interpretation, U.A.R. Amer. Assoc. Petro. Geol. Bull., 52(4), 601-614.

Yuanming, P., and Michael, E. F.,1991. Anadian allanite-(La) and anadian allanite-(Ce) from the Hemlo Gold Deposit, Ontario, Canada. Mineral. Mag., 55(381), 497-507.

جيولوجية وتوزيعات اليورانيوم والثوريوم بمنطقة جبل حمر الراحة،شمال الصحراء الشرقية، مصـــر

أحمد أبو ستيت

يتناول هذا البحث دراسة جيولوجية وبتروجرافية وإشعاعية لمنطقة جبل حمر الراحة، شمال الصحراء الشرقية، مصر. وتبلغ مساحة هذه المنطقة حوالى ١٥٠كم٢ وتقع بين خطى عرض ١٨ ' ٢٧° و٢٦' ٢٧° شمالاً وخطى طول ٤٢' ٣٢° و ٤٨' ٣٢° شرقاً. وتغطى هذه المنطقة بصخور بركانيات الدخان (الأقدم) والجرانيتات الحديثة (السيانوجرانيت) والقواطع (الأحدث).

تمثل بركانيات الدخان قطاع سميك من تتابع طباقى من فيوض متوسطة إلى حامضية التركيب، أما الجرانيتات الحديثة فيمكن تمييزها إلى السيانوجرانيت.

وقد تم مسح هذه المنطقة إشعاعياً باستخدام جهاز أشعة جاما الطيفي المحمول (طراز (UG-130) وقد أظهرت هذه القياسات أن صخور البركانيات الحامضية والجرانيتات الحديثة ذات مستوى عالى من الإشعاع وكذلك محتوى عالى من اليورانيوم والثوريوم. ومن خلال التحليل الراديومترى لعدد ٨ عينات ممثلة لصخور الجرانيتات الحديثة (السيانوجرانيت) ، أتضح أنها تحتوى على يورانيوم يتراوح بين ٩ و ٧٠ جزء من المليون وعلى ثوريوم يتراوح بين ٢٨ و ١١٠ جزء من المليون. كما أوضحت الدراسة أن نسب eTh/eU في صخور السيانوجرانيت المشع أقل من ٢,٢ مما يدل على الإثراء باليورانيوم بالمحاليل السطحية والمحاليل التحت سطحية. و قد أدى انتشار هذه المحاليل خلال الشروخ والصدوع إلى تحرير اليورانيوم من الصخور المحيطة أو من الجرانيتات الحديثة نفسها ثم ترسيبها بعد ذلك فى نطاقات الكسور والصدوع بسبب التبخير أو الإدمصاص على المعادن الطينية وأكاسيد الحديد.

كما أثبتت الدراسات الميكروسكوبية وجود بعض المعادن الإضافية الحاملة لليورانيوم والثوريوم فى صخور السيانوجرانيت مثل معدن الزيركون ومعدن الألنيت.